doi:10.1093/brain/awh683 *Brain* (2006), **129,** 243–255

Neuropathology of fragile X-associated tremor/ataxia syndrome (FXTAS)

C. M. Greco,[1] R. F. Berman,[6] R. M. Martin,[6] F. Tassone,[5,7] P. H. Schwartz,[10] A. Chang,[11] B. D. Trapp,[11] C. Iwahashi,[7] J. Brunberg,[2] J. Grigsby,[8] D. Hessl,[3,4] E. J. Becker,[7] J. Papazian,[5] M. A. Leehey,[9] R. J. Hagerman[4,5] and P. J. Hagerman[5,7]

Departments of [1]Pathology, [2]Radiology, [3]Psychiatry and Behavioral Sciences, [4]Pediatrics and [5]MIND Institute, University of California, Davis, Medical Center, Sacramento, CA, [6]Departments of Neurosurgery and [7]Biochemistry and Molecular Medicine, University of California, Davis, School of Medicine, Davis, CA, Departments of [8]Medicine and [9]Neurology, University of Colorado Health Sciences Center, Denver, CO, [10]Children's Hospital of Orange County Research Institute, Orange, CA and [11]Department of Neurosciences, Lerner Research Institute, Cleveland Clinic Foundation, Cleveland, OH, USA

Correspondence to: Paul J. Hagerman, MD, PhD, Department of Biochemistry and Molecular Medicine, University of California, Davis, School of Medicine, One Shields Avenue, Davis, CA, USA
E-mail: pjhagerman@ucdavis.edu

Fragile X-associated tremor/ataxia syndrome (FXTAS) is an adult-onset neurodegenerative disorder that affects carriers, principally males, of premutation alleles (55–200 CGG repeats) of the fragile X mental retardation 1 (*FMR1*) gene. Clinical features of FXTAS include progressive intention tremor and gait ataxia, accompanied by characteristic white matter abnormalities on MRI. The neuropathological hallmark of FXTAS is an intranuclear inclusion, present in both neurons and astrocytes throughout the CNS. Prior to the current work, the nature of the associations between inclusion loads and molecular measures (e.g. CGG repeat) was not defined. Post-mortem brain and spinal cord tissue has been examined for gross and microscopic pathology in a series of 11 FXTAS cases (males, age 67–87 years at the time of death). Quantitative counts of inclusion numbers were performed in various brain regions in both neurons and astrocytes. Inclusion counts were compared with specific molecular (CGG repeat, *FMR1* mRNA level) and clinical (age of onset, age of death) parameters. In the current series, the three most prominent neuropathological characteristics are (i) significant cerebral and cerebellar white matter disease, (ii) associated astrocytic pathology with dramatically enlarged inclusion-bearing astrocytes prominent in cerebral white matter and (iii) the presence of intranuclear inclusions in both brain and spinal cord. The pattern of white matter pathology is distinct from that associated with hypertensive vascular disease and other diseases of white matter. Spongiosis was present in the middle cerebellar peduncles in seven of the eight cases in which those tissues were available for study. There is inclusion formation in cranial nerve nucleus XII and in autonomic neurons of the spinal cord. The most striking finding is the highly significant association between the number of CGG repeats and the numbers of intranuclear inclusions in both neurons and astrocytes, indicating that the CGG repeat is a powerful predictor of neurological involvement in males, both clinically (age of death) and neuropathologically (number of inclusions).

Keywords: trinucleotide repeat; dementia; RNA toxicity; Parkinson; *FMR1*

Abbreviations: FXTAS = fragile X-associated tremor/ataxia syndrome; GFAP = glial fibrillary acidic protein; MCPs = middle cerebellar peduncles; ROIs = regions of interest

Received July 14, 2005. Revised October 5, 2005. Accepted October 6, 2005. Advance Access published on December 5, 2005

Introduction

Fragile X-associated tremor/ataxia syndrome (FXTAS) is a recently discovered disorder that affects more than one-third of older adult male carriers of premutation alleles (55–200 CGG repeats) of the fragile X mental retardation 1 (*FMR1*) gene (Hagerman *et al.*, 2001; Berry-Kravis *et al.*, 2003; Jacquemont *et al.*, 2003, 2004*b*; Leehey *et al.*, 2003; Hagerman

and Hagerman, 2004). Some female carriers also develop FXTAS (Hagerman *et al.*, 2004; Zuhlke *et al.*, 2004; Berry-Kravis *et al.*, 2005; Jacquemont *et al.*, 2005), although with much lower incidence than males (Berry-Kravis *et al.*, 2003; Jacquemont *et al.*, 2004*b*). In addition to the core features of progressive intention tremor and gait ataxia, affected individuals commonly have parkinsonism, autonomic dysfunction, cognitive decline, emotional problems including disinhibition and apathy, and peripheral neuropathy (Jacquemont *et al.*, 2003, 2004*a*; Bacalman *et al.*, 2005). MRI findings include global brain atrophy and white matter alterations manifested as increased T2 signal intensity in the subcortical regions and in middle cerebellar peduncles (MCPs) (Brunberg *et al.*, 2002), consistent with a previous report of spongiosis in the deep cerebellar white matter (Greco *et al.*, 2002).

Based on a carrier frequency of ~1 in 800 carrier males and 1 in 260 carrier females in the general population (Rousseau *et al.*, 1995; Dombrowski *et al.*, 2002), it is likely that as many as 1 in 3000 males will have a lifetime risk of developing FXTAS. Thus, FXTAS could be a common single-gene cause of tremor, ataxia and cognitive decline among older adults (Hagerman and Hagerman, 2004; Jacquemont *et al.*, 2004*b*). How the clinical and neuropathological features of FXTAS correlate with the size of the CGG repeat within the premutation range is unknown. Such knowledge would improve our understanding of the disease mechanism and provide better estimates of disease prevalence and severity within the general population.

We previously reported neuropathological findings in four males who died with FXTAS (Greco *et al.*, 2002). Those findings included eosinophilic intranuclear inclusions in neurons and astrocytes throughout the cortex and in deep cerebellar nuclei, but not in Purkinje cells of the cerebellum. The inclusions appear as well-delineated, eosinophilic, 2–5 micron spheres that are PAS, silver, tau and synuclein negative, and ubiquitin and αB-crystallin positive (Greco *et al.*, 2002; Iwahashi *et al.*, 2005). To provide a more systematic evaluation of the neuropathological changes in FXTAS and, in particular, to assess the variation in number and distribution of the intranuclear inclusions, we have analysed an additional seven cases of FXTAS post-mortem. The results of this analysis confirm the major histological features of the white matter disease, and establish the presence of inclusions as an essentially constant feature of FXTAS in males. Furthermore, within the current cases, there are highly significant associations between CGG repeat length and both the number of inclusions and the age of death.

Clinical and neuropathological summaries of the current series

Key clinical features of all 11 cases analysed to date are presented in Table 1; the corresponding neuropathological features are presented in Table 2. Cases 1–4 have been presented previously (Greco *et al.*, 2002). The cases were all identified as grandfathers of children with fragile X syndrome. Two cases (10 and 11) are noteworthy for unusual features of involvement. For Case 10, with the most rapid decline to dementia of all of the patients in the current series, neuropathological examination revealed neurofibrillary tangles and neuritic plaques in numbers and distribution consistent with a diagnosis of intermediate stage Alzheimer's disease (NIA-Reagan criteria; Newell *et al.*, 1999), in addition to his diagnosis of FXTAS, as reported previously (Mothersead *et al.*, 2005). This patient demonstrated significant muscle weakness, muscle atrophy and shortness of breath in the late stages of his disease, and became obtunded and died from aspiration pneumonia after choking on liquids. Case 11, with the smallest CGG expansion (65 repeats, determined after death) of this series (Table 1), displayed a very mild phenotype without noticeable tremor. From a clinical perspective, it would have been difficult to make a diagnosis of FXTAS in this case, since no MRI was performed before death, and since neurological symptoms (ataxia) appeared only within 1 year of death. Neuropathological features were also quite mild (Table 2), and although several inclusions were observed in a manual scan of hippocampal neurons, they were quite rare (<1%) and were absent in the astrocytic population. There was no subcortical white matter pathology, nor was there spongiosis in the MCP or deep cerebellar white matter.

Methods

Pathology

Autopsies

Brain autopsies of Cases 5–11 were performed in a standard fashion and in accordance with University of California, Davis, IRB approved protocols. Autopsies of Cases 1–4 were reported in Greco *et al.* (2002). In most cases, one-half of the fresh brain was cut in coronal sections and frozen at −70°C, with the remaining half fixed in 10% formalin. In some cases, the entire brainstem and cerebellum were fixed in formalin for post-mortem MRI studies. After 2 weeks of formalin fixation, hemispheres were cut into 1 cm coronal sections. The brains were routinely sampled to include cerebral cortex, basal ganglia, hippocampus, midbrain, pons, middle cerebellar peduncles, medulla and cerebellum.

Histology and immunochemistry

Tissue blocks were processed for paraffin embedding in a standard fashion. Staining using haematoxylin and eosin (H&E), and luxol fast blue counterstained with periodic acid-Schiff (myelin), were performed according to the standard methods. Staining with silver (modified Bielschowsky) stain for axons was performed on selected cases (Greco *et al.*, 2002). Immunocytochemical staining using anti-ubiquitin, anti-glial fibrillary acidic protein (anti-GFAP), anti-CD68 (KP-1; Dako, Carpenteria, CA, USA), anti-LCA (CD-45; DakoCytomation, Denmark) and anti-neurofilament (Dako) antibodies was performed using methods reported previously (Greco *et al.*, 2002). Dual-label (MBP/ubiquitin) biquitin) immunostaining was performed using the avidin–biotin procedure, with anti-myelin basic protein antibody (SM 194;

Table 1 Clinical and molecular profiles of the eleven cases described in the current study

	1	2	3	4	5	6	7*	8	9	10	11
Age of death	70	78	69	84	67	77	76	75	81	67	87
Age of tremor onset	67	Present	None	70	55	64	None	72	77	61	None
Age of ataxia onset	60	65	64	70	48	65	70	72	65	63	86
Age of cane/ walker use	63	NA	Never	82: Cane 83: Walker	58: Cane	70: Cane 71: Walker	73: Cane 74: Walker	73: Walker	75: Cane 77: Walker	64: Cane 65: Walker	86: Cane 86: Walker
Age of wheelchair use	65.5	NA	Never	83	60	71	75	Never	78	65	Never
FXTAS stage	6	NA	3	6	5	6	6	5	5	6	NA
Cognitive deficits	Dementia	Memory loss	Memory loss	Memory loss	Memory loss	Dementia	Dementia	Memory loss	Dementia	Dementia	Word retrieval difficulties
Sensory/motor dysfunction	LE weakness	NA	LE weakness	LE weakness	LE weakness & sensory loss	LE weakness	LE weakness & sensory loss	None	None	LE sensory loss	Rt LE sensory loss (post-CVA)
Parkinsonism	NA	Cogwheeling	None	Resting tremor, bradykinesia, stiffness, hypomimia	NA	Resting tremor	Masked facies	None	None	None	None
MRI findings	NA	Mild CCA (on CT)	MCP+; CCA; WMD	CCA (on CT)	NA	MCP+; CCA; WMD	MCP+	NA due to pacemaker	MCP+; CCA; WMD	MCP+; CCA; WMD	NA
Emotional symptoms	Depression	NA	Depression, anger outbursts, anxiety	NA	Depression, anxiety	Anger outbursts	NA	NA	Depression, mood instability, psychotic episodes	Depression, anxiety, anger outbursts	None
Dysphagia	Y	Y	N	Y	N	Y	N	NA	N	Y	NA
Hypertension	N	NA	Y	N	Y	Y	Y	N	Y	Y	Y
Incontinence	Y	NA	N	N	Y	Y	N	N	Y	Y	Y
Impotence	Y	NA	N	N	NA	Y	N	N	Y	N	NA
Other medical issues	Type II DM; CAD; COPD; MI	NA	Colon ca; CHF	Mitral valve replacement; pacemaker	Bladder ca; prostate ca; CAD; atrial fib; CVA	RA; CHF; angioplasty & stent	CHF; sick sinus syndrome; MI × 2 triple bypass; pacemaker	Pacemaker; CHF	Triple bypass; deafness in L ear; malignant tachycardia; AS	Nosebleeds; polyps; prostatectomy	CVA; hypothyroid; BPH; osteoarthritis; DVT; irritable bladder
CGG repeats	113	80	80	71	105	77	88	92	88	93	65
FMR1 mRNA (SEM)	3.8 (0.13)	NA	NA	NA	6.72 (0.92)	3.87 (0.58)	7.0 (0.47)	2.27 (0.45)	4.13 (0.49)	3.46 (0.29)	NA
% FMRP	62	NA	NA	NA	63	74	68	89	73	89	NA

NA = not available; WMD = white matter disease; CCA = cortical and cerebellar atrophy; LE = lower extremity; RA = rheumatoid arthritis; OS = osteoarthritis; DM = diabetes mellitus; ca = cancer; CHF = congestive heart failure; MI = myocardial infarction; COPD = chronic obstructive pulmonary disease; CAD = coronary artery disease; AS = aortic stenosis; CVA = cerebral vascular accident; DVT = deep vein thrombosis; BPH = benign prostatic hypertrophy. FXTAS stage: stages 0/1, uninvolved/equivocal involvement; stage 2, definite tremor or ataxia not interfering with ADLs; stage 3, tremor or ataxia interfering with ADLs; stage 4, use of a cane or walker; stage 5, use of a wheelchair; stage 6, bedridden (Bacalman *et al*., 2005).
*Brother of Case 6.

Table 2 Summary of the neuropathology in post-mortem brain tissue from 11 males with FXTAS

Case	Intranuclear (neuronal and astrocytic) inclusions	Quantitative inclusion counts	Inclusions present in ependyma and choroid plexus	Cerebral (gross) white matter pathology	Periventricular pallor (microscopic)	Basal ganglia vascular changes	Cerebral white matter hyalinopathy	Patchy white matter axon and myelin loss	MCP spongiosis	Cerebellar Purkinje cell dropout	Cerebellar white matter spongiosis	Inclusions in CN XII nucleus	Spinal cord autonomic inclusions	Other pathology
1	Yes	Yes	Yes	NA	NA	–	–	+	NA	+	Yes	NA	NA	
2	Yes	NA	Yes	–	–	PVW	–	NA	Yes	+	Yes	NA	No	
3	Yes	NA	NA	NA	NA	NA	NA	NA	NA	NA	NA	NA	NA	Limited to cortical sample w/freezing artefact
4	Yes	NA	NA	NA	NA	NA	NA	NA	NA	NA	NA	NA	NA	Extensive freezing/ fixation artefact
5	Yes	Yes	Yes	–	–	PVW	+	+	Yes	–	Yes	No	Yes	
6	Yes	Yes	Yes	+++	–	PVW	–	++	Yes	+++	Yes	Yes	Yes	Fixation artefacts
7	Yes	Yes	Yes	+++	NA	–	+	++	Yes	+	Yes	Yes	Yes	
8	Yes	Yes	Yes	See (other path)	+	PVW	++	+	NA	++	Yes	No	Yes	Multiple infarcts, R MCP angioma, L MCP infarcts
9	Yes	Yes	Yes	–	–	–	+	+	Yes	+++	Yes	No	NA	Inclusions in Purkinje cell nuclei
10	Yes	Yes	Yes	–	+/–	–	–	+	Yes	+	Yes	NA	NA	Intermediate stage Alzheimer's disease
11	Rare	Yes	No	–	–	PVW	++	–	No	–	No	No	NA	A few putaminal remote microinfarcts

All scales of severity: normal or minimal abnormality (–), mild (+), moderate (++), extensive/severe (+++). Only cranial nerve 12 (CN XII) was sampled. NA, tissue not available for analysis, either because specific samples were unavailable or because fixation artefacts precluded further analysis. PVW, perivascular widening. Reference for NIA-Reagan criteria (Newell *et al.*, 1999).

Sternberger Monoclonals, Baltimore, MD, USA) visualized with DAB and the anti-ubiquitin antibody (Dako, Glostrup, Denmark) visualized with Vector Nova Red Substrate (Vector Laboratories, Burlingame, CA, USA). Appropriate positive and negative controls were employed for each antibody.

Intranuclear inclusion and cell counts

The percentages of neurons and astrocytes harbouring intranuclear inclusions were determined for frontal cortex, hippocampus and the ventral pontine region. Tissue blocks of frontal cortex, hippocampus and pons were obtained from 8 out of 11 male FXTAS patients (Cases 3, 4 and 6 had fixation artefacts that precluded further analysis of neuronal densities/inclusion counts) and 10 normal (no neurological disease), age-matched control subjects (5 male and 5 female). Control males were chosen to match the average age of the carrier male group. Ages of the control males ranged from 60 to 76 years. The analysis of cell counts and neuronal densities utilized those cases that had sufficient tissue for serial sectioning and were free of severe fixation artefacts that precluded stereological evaluation. Control cases were extracted from the pathology files at the University of California, Davis Medical Center Department of Pathology, in accordance with a UC Davis approved IRB protocol. Brain tissue samples were cut from the same region and, to the extent possible, in the same orientation to facilitate histological analyses. Tissue was paraffin embedded, sectioned at 10 μm and stained with H&E. Every fifth section was used for histological analysis, for a total of three tissue sections for each brain region.

Regions of interest (ROIs) were then outlined within the frontal cortex, hippocampus and ventral pontine region using a Nikon E600 microscope; an unbiased and random sample of neurons and astrocytes within these ROIs was used to estimate the percentage of cells with intranuclear inclusions. In the hippocampus, with well-defined morphological boundaries, three ROIs were outlined (CA1, granule cell layer and hilus). In the frontal cortex and ventral pontine region, well-defined ROIs could not be generated using cytoarchitectonic boundaries; therefore, ROIs were defined as a constant area within cortical grey and white matter and in the pontine nuclei. The area of the ROI outlined in the grey matter was set to 1.8×10^7 μm^2, and encompassed cortical layers II–VI, while an area of 1.2×10^7 μm^2 was used in the cortical white matter ROI. The pontine ROI was set to an area of 4.0×10^6 μm^2.

Cell identification within ROIs was carried out primarily on H&E stained sections using standard morphological criteria. Neurons were identified by their size; by large, centrally placed, round-to-ovoid nuclei with dense heterochromatin and nucleoli; and by their abundant cytoplasm. Astrocytes were identified by their irregular, ovoid nuclei with light euchromatin, their lack of nucleoli and the absence of cytoplasm. In most cases, neuronal and astrocytic nuclei were easily distinguished by the above criteria, with the added feature of astrocyte location (perivascular or immediately adjacent to neuronal cytoplasmic borders). In the small number of instances where cortical granular neuronal nuclei might be of the same size as astrocytic nuclei, and did not show nucleoli or obvious cytoplasmic borders, we relied on the chromatin pattern of the nucleus to distinguish between the cell types. These distinctions were also verified in separate GFAP staining experiments. Neurons bearing intranuclear inclusions were not otherwise structurally altered. Astrocytic nuclei containing inclusions were increased in size and showed a clear halo around the inclusion (Greco *et al.*, 2002). Oligodendroglial nuclei were distinguished as small, round, hyperchromatic nuclei that showed neither nucleoli nor cytoplasm. In addition to their diffuse distribution throughout white matter, oligodendroglia can closely oppose neuronal cell bodies. Eosinophilic intranuclear inclusions were identified as described previously (Greco *et al.*, 2002).

The optical fractionator probe in the Stereo Investigator software (Microbrightfield, Inc., Williston, VT) was used to overlay sampling grids across each ROI. Counting frames were then defined within the sampling grids, and neurons and astrocytes with and without inclusions that fell within the counting frames were counted using a ×100 oil immersion objective. Counting frames were set at 90 μm × 90 μm except for the hippocampal granule cell layer where they were 50 μm × 50 μm due to the increased granule cell density. The individual ratios of the number of neurons and astrocytes with inclusions to the total sample of each were determined (i.e. number with inclusions/total sample), and were then used to calculate the percentage of each cell type with inclusions (Tables 3–5). In addition, estimates of neuronal and astrocyte densities (cells/mm^3) within cortical ROIs were calculated from optical fractionator cell counts and Cavalieri volume measurements.

Because generalized brain atrophy has been associated with FXTAS, average cortical thickness was directly measured in the grey matter of the frontal cortex using the distance measurement functions of the Stereo Investigator software. Briefly, for each tissue section, three distinct lines were drawn from and perpendicular to the cortical surface, extending medially to the grey matter/white matter interface. The average lengths (μm) of the lines were used to estimate mean cortical thickness.

Statistical analyses

Estimates of neuronal and astrocytic densities in cortex and cortical grey matter thickness were compared between FXTAS patients and controls by analysis of variance (SPSS Inc, Chicago, IL, USA). Correlations were calculated between histological findings, molecular measures (e.g. number of CGG repeats, levels of *FMR1* mRNA and FMRP) and clinical findings (e.g. age of onset of ataxia, age of death) using Spearman's rho (SPSS). For multiple correlations, the alpha levels for minimum statistical significance were adjusted to reduce the possibility of type I errors (i.e. familywise error rate) using Bonferroni's correction (Curtin and Schulz, 1998), with separate (familywise) groupings of histological, molecular and clinical correlations. Molecular/inclusion correlations and statistical analyses were performed separately for each brain region (i.e. frontal, cortical grey, hippocampal CA1, etc.). The Benjamini–Hochberg procedure was also used to control for false discovery rate (Benjamini and Hochberg, 1995). With both procedures, adjusted alpha levels ranged from 0.008 to 0.50 and yielded an identical set of statistically significant correlations for the data presented in this study.

Molecular measures

Genomic DNA and total RNA were isolated from peripheral blood leucocytes obtained prior to death, and from post-mortem sections of ~500 mg of brain tissue using standard methods (Puregene and Purescript Kits; Gentra Inc., Minneapolis, MN, USA). Southern blot- and PCR-based genotyping, and *FMR1* mRNA quantification, were performed as described previously (Tassone *et al.*, 2000*b*, 2004). Immunocytochemical detection of FMRP was performed on blood smears as described previously (Tassone *et al.*, 1999).

Table 3 Frontal cortex histological results

Subject	Frontal cortex										Cortical thickness (μm)
	Grey matter				White matter				Grey cortex densities		
	Neurons	%	Astrocytes	%	Neurons	%	Astrocytes	%	Neurons/mm^3	Astrocytes/mm^3	
Controls											
19	0/386	0.0	0/187	0.0	0/0	NA	0/366	0.0	33 500	16 229	2857
26	0/359	0.0	0/270	0.0	0/14	0.0	0/423	0.0	31 165	23 439	4430
51	0/419	0.0	0/360	0.0	0/17	0.0	0/331	0.0	36 360	31 240	2880
65	0/387	0.0	0/223	0.0	NA		NA		33 598	19 360	2567
67	0/392	0.0	0/252	0.0	0/1	0.0	0/176	0.0	34 024	21 872	3111
73	0/492	0.0	0/265	0.0	0/34	0.0	0/213	0.0	42 723	23 012	2987
74	0/221	0.0	0/221	0.0	0/21	0.0	0/191	0.0	19 190	19 190	3009
75	0/262	0.0	0/252	0.0	0/5	0.0	0/382	0.0	22 736	21 868	3241
93	0/330	0.0	0/230	0.0	0/8	0.0	0/344	0.0	28 658	19 974	3310
Ave ± SEM		0.0		0.0		0.0		0.0	31 329 ± 2356	21 798 ± 1396	3155 ± 176
FXTAS (Cases)											
1	23/376	6.9	43/122	35.2	1/2	50.0	20/214	9.3	32 649	10 594	4121
5	12/304	3.9	32/163	19.6	1/10	10.0	22/278	7.9	26 398	14 154	3518
6	5/332	1.5	45/346	13.0	2/9	22.2	3/248	1.2	28 821	30 036	NA
7	7/375	1.9	52/347	15.0	0/0	NA	1/197	0.5	32 540	30 110	2621
8	23/401	5.7	61/284	21.5	1/10	10.0	42/298	14.1	34 816	24 658	3657
9	16/494	3.2	30/280	10.7	2/7	28.6	9/276	3.3	42 896	24 314	3183
10	52/430	12.1	70/378	18.5	1/3	33.3	28/690	4.1	37 353	32 836	2936
11	0/412	0.0	0/261	0.0	0/2	0.0	0/288	0.0	35 796	22 677	3042
Ave ± SEM		4.4		16.7		22.0		5.0	33 909 ± 1807	23 672 ± 2771	3297 ± 190

Summary of the numbers of neurons and astrocytes with intranuclear inclusions in frontal cortex. Results are expressed as ratios of the number of neurons and astrocytes with inclusions per total number counted, and as a percentage (%) of neurons and astrocytes with intranuclear inclusions. Results for grey and white matter are presented separately. Also shown is a summary of measured neuronal and astrocytic densities in the frontal cortical grey matter, expressed as the number of neurons/astrocytes per cubic millimetre. Measurements of cortical thickness are also summarized. NA = not available.

Results

Neuropathological examination of 11 cases confirms and further defines the prominent cortical and subcortical white matter pathology associated with FXTAS

A prominent feature of the brains within this series was the presence of white matter disease in broad distribution within the cerebrum (Fig. 1) and cerebellum. On gross examination, for those cases where intact hemispheres or whole brains were available (Cases 1, 2 and 5–11), there was mild to moderate cortical atrophy and ventriculomegaly. Brain weights were within expected normal limits (1100–1700 g; average 1400 g), except for Case 6 (JS), where the weight was greatly decreased due to preservation in a non-formalin fixative. One case showed severe, gross white matter abnormalities (Case 7). Microscopic examination of cerebral white matter showed varying degrees of a similar pathological process in all cases where this tissue was available (e.g. Figs 2 and 3) except for Case 11, where only rare inclusions were observed. Of particular note was the presence of dramatically enlarged GFAP-positive astrocytes in white matter. Other abnormal features included variable degrees of spongiosis in subcortical and deep white matter, with corresponding axonal loss on Bielschowsky or neurofilament stain and myelin pallor on LFB-PAS stain. Glial cell loss varied in degree of severity with the above changes, and, uncommonly, axonal swellings (best observed with neurofilament staining) were identified (Fig. 4). Abnormal MCPs and deep cerebellar white matter disease were present in all cases where these tissues were available (except for Case 11), and demonstrated spongiosis with rare axonal spheroids and myelin pallor on LFB-PAS stain. Purkinje cell loss ranged from mild to severe, and was accompanied by corresponding Bergmann gliosis; cases showing moderate to severe loss of Purkinje cells were considered abnormal for age.

The second prominent feature of the brains was the widespread presence of intranuclear neuronal and astroglial inclusions, as described previously (Greco *et al.*, 2002). These were seen diffusely in cortex, basal ganglia, thalamus, substantia nigra, inferior olivary and dentate nuclei, generally sparing only cerebellar Purkinje cells (rare Purkinje cell inclusions were identified in Case 9). Importantly, inclusions could not be found in the oligodendroglial population; double-immunolabelled (MBP/ubiquitin) sections, for oligodendroglia and inclusions, respectively, failed to detect any inclusions in over 600 oligodendroglial nuclei counted (Fig. 5). Intranuclear inclusions were also rare in pontine

Table 4 Hippocampal histological results

Subject	Hippocampus											
	Pyramidal				Granular cell layer				Hilus			
	Neurons	%	Astrocytes	%	Neurons	%	Astrocytes	%	Neurons	%	Astrocytes	%
Controls												
09	0/152	0.0	0/140	0.0	0/364	0.0	0/53	0.0	0/120	0.0	0/254	0.0
19	0/98	0.0	0/124	0.0	0/517	0.0	0/43	0.0	0/116	0.0	0/350	0.0
26	0/158	0.0	0/170	0.0	0/382	0.0	0/32	0.0	0/84	0.0	0/169	0.0
51	0/117	0.0	0/207	0.0	0/449	0.0	0/32	0.0	0/63	0.0	0/291	0.0
65	0/133	0.0	0/149	0.0	0/394	0.0	0/41	0.0	0/70	0.0	0/120	0.0
67	0/95	0.0	0/118	0.0	0/623	0.0	0/59	0.0	0/80	0.0	0/282	0.0
73	0/125	0.0	0/150	0.0	0/484	0.0	0/29	0.0	0/70	0.0	0/218	0.0
74	0/107	0.0	0/83	0.0	0/378	0.0	0/29	0.0	0/111	0.0	0/180	0.0
75	NA		NA		0/276	0.0	0/38	0.0	0/75	0.0	0/384	0.0
93	NA		NA		NA		NA		0/81	0.0	0/224	0.0
Average		0.0		0.0		0.0		0.0		0.0		0.0
FXTAS (Cases)												
1	29/152	19.1	24/74	32.4	44/594	7.4	12/28	42.9	8/91	8.8	49/186	26.3
5	13/80	16.3	4/51	7.8	7/354	2.0	5/16	31.3	7/73	9.6	67/163	41.1
6	5/81	6.2	8/157	5.1	8/1109	0.7	10/40	25.0	30/153	19.6	93/327	28.4
7	5/97	5.2	8/129	6.2	14/1002	1.4	5/23	21.7	2/72	2.8	53/217	24.4
8	19/131	14.5	27/272	9.9	11/675	1.6	24/55	43.6	27/126	21.4	116/403	28.8
10	17/180	9.4	11/101	10.9	13/834	1.6	8/37	21.6	24/115	20.9	124/253	49.0
11	0/158	0.0	0/127	0.0	0/651	0.0	0/43	0.0	0/209	0.0	0/278	0.0
Average		10.1		10.3		2.1		26.6		11.9		28.3

Number of neurons and astrocytes with intracellular inclusions in the CA1 pyramidal cell layer, granule cell layer and hilus. The numbers of inclusions are expressed as a ratio of cells with inclusions per total number of cells counted, and also as percentage (%) of neurons and astrocytes with inclusions. NA = not available.

Table 5 Pontine nuclei histological results

Subject	Neurons	%	Astrocytes	%
Controls				
09	0/218	0.0	0/65	0.0
19	0/128	0.0	0/125	0.0
26	0/142	0.0	0/156	0.0
51	0/210	0.0	0/132	0.0
65	0/113	0.0	0/88	0.0
67	0/179	0.0	0/91	0.0
73	0/207	0.0	0/105	0.0
74	0/118	0.0	0/147	0.0
75	0/168	0.0	0/165	0.0
93	0/107	0.0	0/110	0.0
Average		0.0		0.0
FXTAS (Cases)				
1	0/166	0.0	15/160	9.4
5	1/104	1.0	25/106	23.6
6	0/235	0.0	26/132	19.7
7	0/104	0.0	32/136	23.5
8	0/219	0.0	41/128	32.0
9	0/197	0.0	12/72	16.7
Average		0.2		20.8

Number of neurons and astrocytes in the pons with intranuclear inclusions. Counts are expressed as number of cells with inclusions per total number of cells counted, and also as the percentage (%) of cells with inclusions.

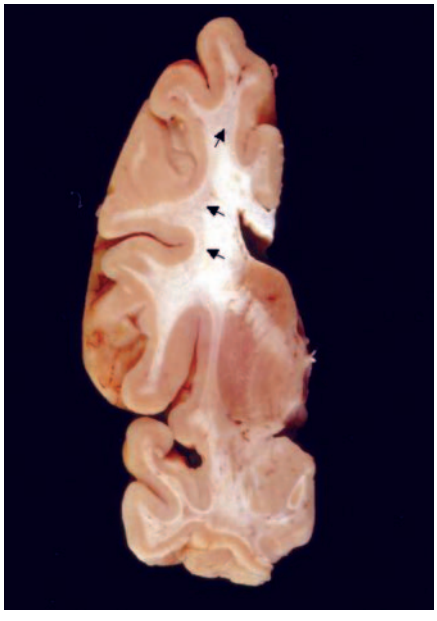

Fig. 1 Coronal section of formalin-fixed brain (Case 7). This case showed severely affected cerebral white matter both grossly and microscopically. Involvement appears as subcortical regions of pale grey discolouration (arrows). These changes were present throughout the cerebral white matter. Note that periventricular white matter is spared.

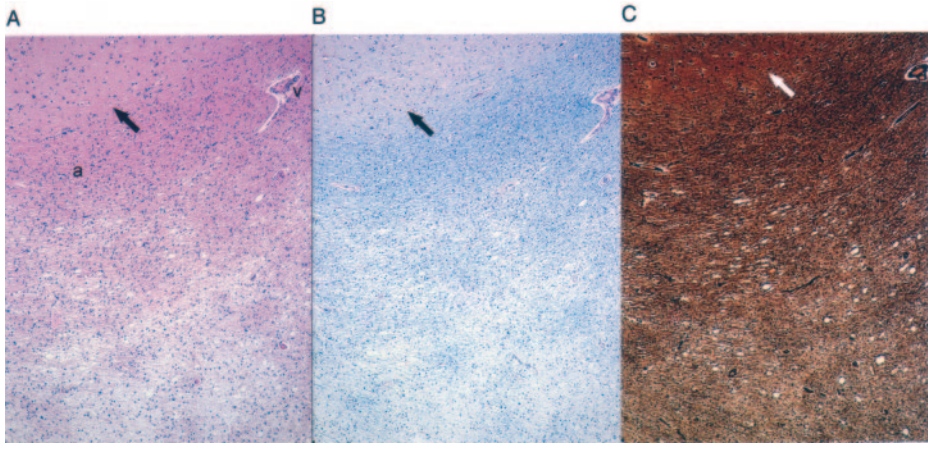

Fig. 2 Cerebral white matter from Case 7, showing (**A**) gradations of spongiosis and parenchymal pallor in subcortical white matter. Note the lack of these changes around vessel (v). Arcuate fibres (a) in this view show little involvement (H&E stain, ×40). (**B**) Corresponding myelin loss is seen on LFP-PAS stain (×40). (**C**) Bielschowsky stain demonstrates axonal loss in the same area (×40). Grey/white matter junction is indicated by arrows.

neurons, although they were frequently observed in pontine astrocytes. Inclusions were easily identifiable in all cases (Cases 1 through 10) except Case 11 (smallest CGG repeat expansion), where only a few neuronal inclusions were detected by direct visualization of ubiquitin immunostained slides. In Cases 1, 2 and 5–10, ependymal and choroid plexus nuclei also showed intranuclear inclusions. Intranuclear inclusions were identifiable in cranial nerve nucleus XII for Cases 6 and 7, 2 out of 6 of the cases where appropriate tissue was available (Cases 5–9 and 11). In Cases 2 and 5–8, for which spinal cord was available, astrocytic intranuclear inclusions were diffusely present in all cases; intranuclear inclusions were identified in autonomic neurons, but not motor neurons, in Cases 5–8 (4 out of 5 cases).

Histological (stereological) findings establish a relationship between CGG repeat length and the numbers of inclusions among cases of FXTAS

The number of neurons and astrocytes with intranuclear inclusions (actual counts and percentages) are presented in Tables 3–5 for cerebral cortex, hippocampus and the ventral pontine region, respectively. No inclusions in neurons or astrocytes were observed for any of the control subjects, and no inclusions were observed in the cytoplasm of neural cells. Furthermore, no intranuclear inclusions were seen by stereological analysis (H&E) for the subject with the lowest CGG repeat expansion (Case 11; 65 CGG repeats). In general, more intranuclear inclusions were observed in astrocytes than in neurons (the hippocampal CA1 subregion was an exception), although there was a great deal of variability across subjects. For example, as shown in Table 3, the mean percentage of neurons with inclusions for cortical grey matter was 4.4% (range 0–12.1%), whereas 16.7% (range 0–35.2%) of cortical astrocytes possessed inclusions.

Analysis of molecular correlation with inclusion counts

A series of correlations (Spearman's rho) were calculated between histological findings and molecular measures (e.g number of CGG repeats, levels of *FMR1* mRNA and FMRP). Representative plots from these correlations are displayed in Fig. 6. Significant correlations between the percentage of neurons with inclusions and the number of CGG repeats were found for several brain regions, including cortical grey matter (rho = 0.874, $P = 0.005$), CA1 pyramidal neurons in hippocampus (rho = 0.929, $P = 0.003$) and hippocampal granule cells (rho = 0.964, $P < 0.001$). Similar correlations between the number of CGG repeats and the percentage of astrocytes with inclusions were significant in the cortical grey matter (rho = 0.886, $P = 0.003$), the CA1 subregion of the hippocampus (rho = 0.893, $P = 0.007$) and the cortical white matter (rho = 0.814, $P = 0.01$). Correlations between number of inclusions and CGG repeats for the remaining brain regions demonstrated similar trends, but, presumably due to the small numbers of inclusions, did not reach statistical significance.

Significant inter-cell-type correlations were also observed for the percentage of neurons versus astrocytes with inclusions in cortical grey matter (rho = 0.786, $P = 0.02$), hilus (rho = 0.821, $P = 0.02$) and in the CA1 region of the hippocampus (rho = 0.821, $P = 0.02$); the comparison only approached significance in the granule cell layer (rho = 0.750, $P = 0.05$).

Although there were apparent correlations between the percentage of hilar neurons with inclusions and levels of *FMR1* mRNA (rho = −0.829, $P = 0.04$) and between the percentage of inclusion-bearing hilar neurons and levels of FMRP (rho = 0.812, $P = 0.05$), these correlations were no longer statistically significant following correction for multiple comparisons. Correlations between percentage inclusions and peripheral blood leucocyte *FMR1* mRNA or FMRP levels in the other brain regions were not statistically significant. This last observation is not surprising in view of

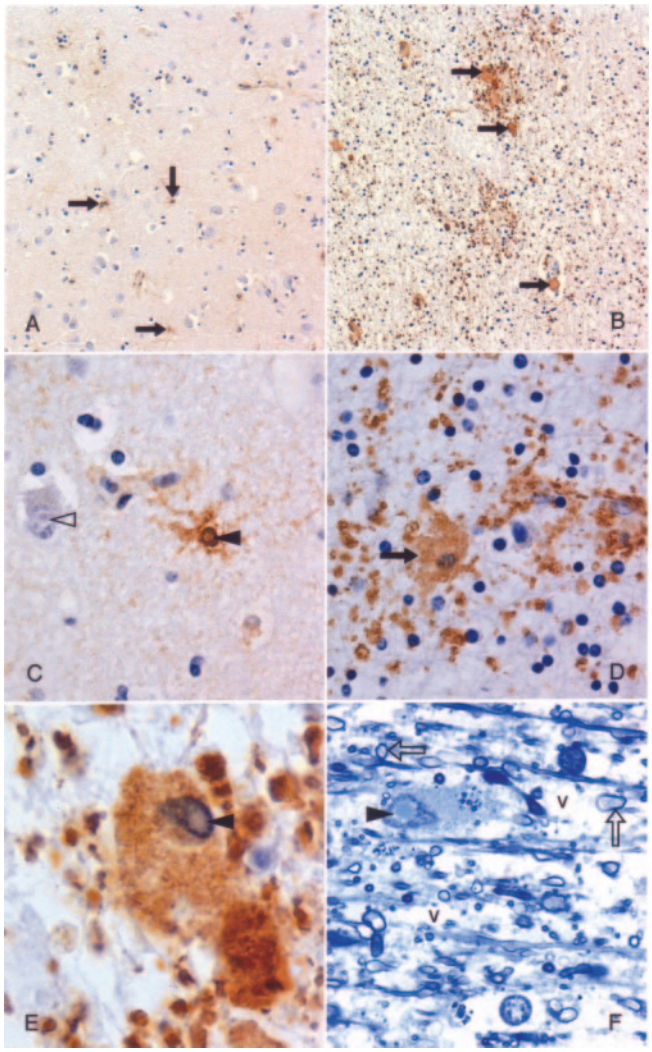

Fig. 3 Astrocytic involvement in grey and white matter (Case 7) (**A**) Scattered, hypertrophied, protoplasmic astrocytes in cortical grey matter (arrows) (×100). (**B**) Subcortical white matter shows, by comparison, large numbers of dramatically enlarged, fibrillary astrocytes (arrows); granular deposits represent hypertrophied astrocytic processes (×100). (**C**) Neuronal (open arrowhead) and astrocytic (closed arrowhead) intranuclear inclusions in cortical grey matter (×400). (**D**) Hypertrophied fibrillary astrocyte in the white matter (×400). (**E**) Remarkably enlarged, inclusion-bearing (arrowhead) astrocyte in the subcortical white matter (×1000). (**A**–**E**) Paraffin-embedded tissue, GFAP immunostained. *Note*: LCA and CD68 immunostaining was negative. (**F**) Similar inclusion-bearing (arrowhead) astrocyte in resin-embedded white matter showing associated spongiosis/vacuolar change (v). Myelinated axons are also indicated (arrows). Formalin-fixed tissue was subsequently fixed in glutaraldehyde solution; methylene blue stain, ×1000.

the large differences between expression levels in brain and blood, and the dramatic region-specific differences in *FMR1* mRNA levels in brain (Tassone *et al.*, 2004).

Analysis of clinical correlations with inclusion counts

The most striking clinical–molecular correlation (Fig. 7) is the significant decrease in age of death with increasing CGG repeat length ($n = 10$; rho = −0.896; $P < 0.001$). Age of tremor onset was not significantly correlated with CGG repeat length, and the initial negative correlation between age of ataxia and CGG repeat length was not significant after correction for multiple outcomes (rho = −0.663, $P = 0.03$). The correlation between the age of onset of ataxia and age of death was significant (rho = 0.747, $P = 0.008$), but not age of tremor onset with age of death (rho = 0.739, $P = 0.06$). The following six correlations were significant before, but not after, correction for multiple outcomes was carried out: negative correlations between the age of death and the percentages of inclusion-bearing neurons in subregions of the hippocampus (granule cell layer: rho = −0.793, $P = 0.03$; CA1: rho = −0.757, $P = 0.05$) and frontal cortical grey matter (rho −0.826, $P = 0.01$) and negative correlations between age of death and the percentages of inclusion-bearing astrocytes in subregions of the hippocampus (hilus: rho = −0.811, $P = 0.03$; CA1: rho = −0.793, $P = 0.03$) and frontal cortical grey matter (rho = −0.802, $P = 0.02$).

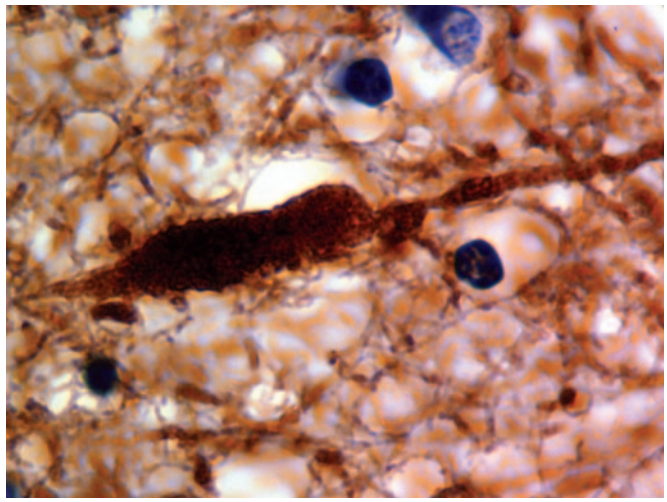

Fig. 4 A single axon in cerebral white matter (Case 7) demonstrating focal swelling. This type of axonal pathology was uncommon (×1000). Neurofilament staining.

Discussion

The current study provides a description of the degenerative cerebral white matter disease that corresponds to previously described MRI changes in FXTAS (Hagerman *et al.*, 2001; Brunberg *et al.*, 2002; Jacquemont *et al.*, 2003; Leehey *et al.*, 2003). Histological changes in cerebral white matter of individuals with FXTAS are distinct from those seen with ischaemia, hypertension, multiple sclerosis, gliosis associated with chronic inflammatory diseases, and cerebral autosomal dominant arteriopathy with subcortical infarcts and leucoencephalopathy (CADASIL) (Kalimo *et al.*, 1999). Given the patchy loss of axons, myelin and attending glia in FXTAS, we postulate neuronal and/or glial dysfunction as causal or contributory in the face of normal cortical thickness and neuronal

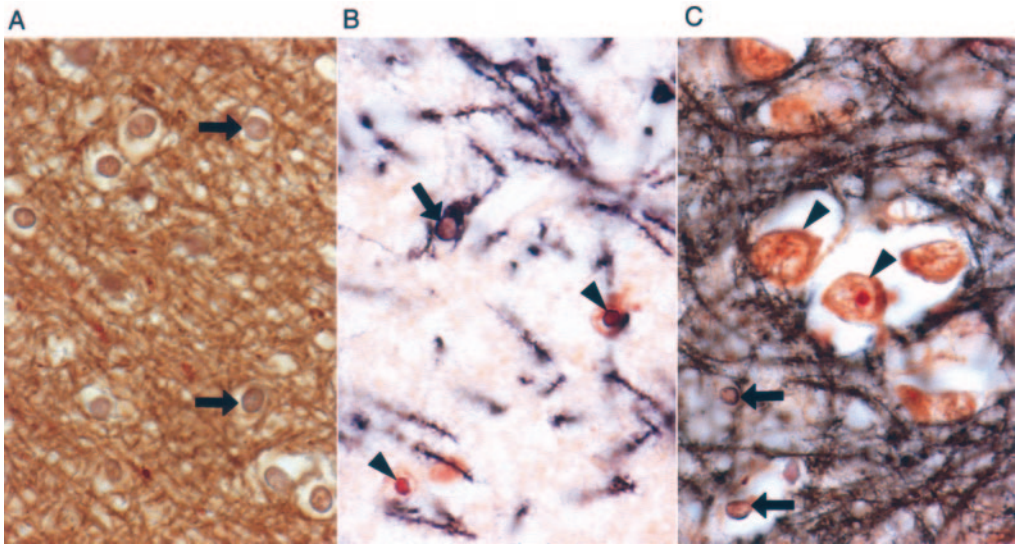

Fig. 5 Examination of oligodendroglial nuclei in white and grey matter (Case 1) for the presence of intranuclear inclusions. (**A**) White matter, with many oligodendroglial nuclei (arrows), all devoid of inclusions. (**B**) Grey matter, demonstrating inclusions in astrocytic nuclei (arrowheads), but not in an oligodendroglial nucleus (arrow). Note the cytoplasmic staining of oligodendroglial cytoplasm for myelin basic protein (MBP); dark brown reaction product. (**C**) Cortical grey matter displaying a cluster of neurons with and without inclusions (arrowheads) and several oligodendroglial nuclei without inclusions (arrows). All sections were double-immunostained for MBP (dark brown) and ubiquitin (red stain) (×630).

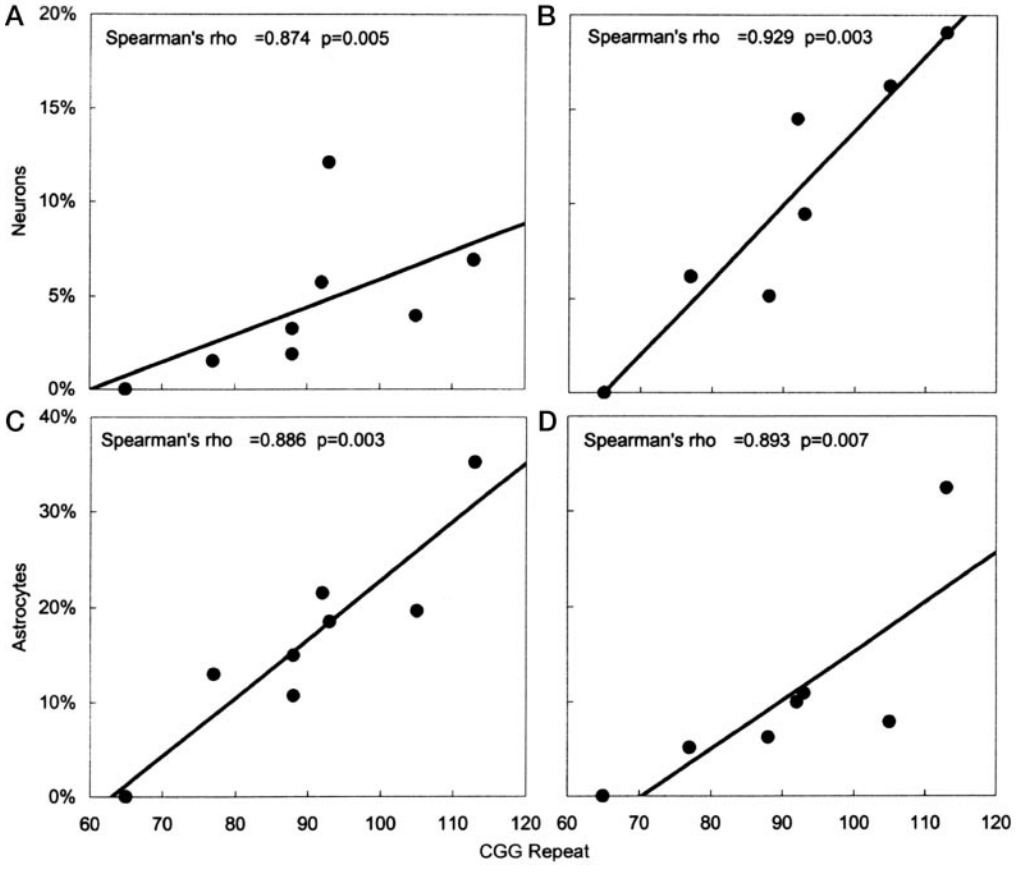

Fig. 6 Scatterplots demonstrating significant correlations between CGG trinucleotide repeat number and the percentage of neurons and astrocytes with intranuclear inclusions. Frontal cortical grey matter neurons (**A**) and astrocytes (**C**). Hippocampal neurons (**B**) and astrocytes (**D**) of the CA1 pyramidal region. Spearman's rho values and *P*-values are given for each plot.

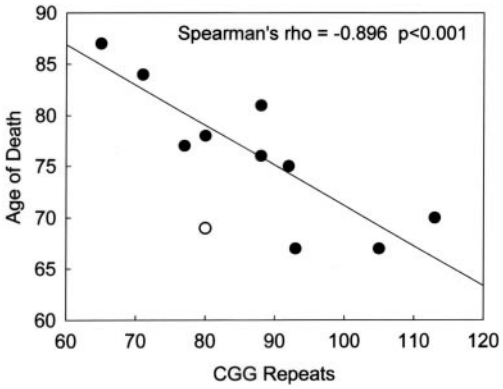

Fig. 7 Negative correlation between the age of death and CGG trinucleotide repeat number for 10 male FXTAS patients (filled circles). The single open circle was not included in the regression since that individual (Case 3) died of drowning (Greco *et al.*, 2002); inclusion of the latter case would still have resulted in a highly significant correlation ($P = 0.005$).

counts, as compared with normal controls. Seven of eight cases with MCP tissue available for analysis (none was available for three cases) showed spongiosis. The MCP is the major afferent pathway into the cerebellum from the pons, predominately arising from pontine neurons. We hypothesize that degenerative changes in the peduncles reflect early damage to the pontine neurons or afferents to those neurons. Purkinje cell dropout, greater than normal ageing in all cases, except Case 11, where cerebellar cortical tissue was available for examination, may be secondary to the diminished input from the pontine neurons or from a more direct toxic RNA effect in the Purkinje cells (Greco *et al.*, 2002; Hagerman and Hagerman, 2004). The deep cerebellar white matter spongiosis, which includes both axonal and myelin loss, may reflect involvement of both afferent and efferent axonal fibres.

In this regard, it is interesting that there is a relative paucity of inclusions in the pontine neurons. However, in light of a trend towards reduced pontine volume, we do not consider the small numbers of inclusions to be a sign of sparing of those neurons. Indeed, inclusions are only rarely observed in Purkinje cells, although that cell population suffers substantial loss in FXTAS cases.

Pathological characterization of cerebral white matter disease shows clearly identifiable abnormalities in 6 out of 7 cases (7 out of 11 cases had sufficient cerebral white matter available for the analysis). These changes range from microscopic white matter pallor to severe white matter degeneration, primarily in the subcortical white matter, with involvement of arcuate fibres and sparing of periventricular white matter. The involved areas showed varying degrees of spongiosis with both myelin and axonal loss, although we have not as yet assessed the relative degrees of axonal and myelin pathology. This pattern of white matter pathology is distinct from that associated with hypertensive vascular disease, which characteristically involves basal ganglia to a greater degree than cerebral white matter and does not involve arcuate fibres. Pathological features seen with hypertension usually include arterial wall hyalinosis, widened perivascular spaces and parenchymal rarefaction around the abnormal small arteries and arterioles. While mild vessel wall changes were present in cerebral white matter in nearly all of our cases, such changes were not accompanied by perivascular parenchymal rarefaction. Vessels of the basal ganglia were spared of hypertensive changes except in Case 5, which had pathological changes attributable to hypertensive cardiovascular disease in the form of multiple cerebral infarcts.

There is clear evidence of inclusion formation in cranial nerve nucleus XII; other cranial nerve nuclei were examined in our routine sections, but did not show inclusions. We plan further examination of brainstem nuclei with serial sections to further document autonomic involvement in FXTAS. Inclusions were also observed in autonomic neurons of the spinal cord, with sparing of the motor neurons of the spinal cord. These observations are consistent with the frequent occurrence of autonomic dysfunction among cases of FXTAS. Such involvement can include orthostatic hypotension, hypertension, impotence and incontinence of bowel and bladder (Hagerman *et al.*, 2001; Jacquemont *et al.*, 2003, 2004*a*). Involvement of cranial nerve XII is consistent with swallowing problems in advanced FXTAS, with choking and aspiration pneumonia contributing to death in some cases.

The psychiatric problems (e.g. depression, anxiety and mood instability/outburst behaviour) encountered by FXTAS patients are also common in the current series (Bacalman *et al.*, 2005). This association is likely related to the significant involvement of the limbic system with prominent inclusion formation in the hippocampus. High levels of *FMR1* mRNA have previously been demonstrated in the hippocampus (Tassone *et al.*, 2004). While cognitive impairment in FXTAS is consistent with the neuropathological findings reported for this series of cases, the broad distribution of inclusions and white matter disease, and the substantial loss of cerebellar Purkinje cells, preclude the association of cognitive deficits with any single factor or locus.

Cognitively, individuals with FXTAS typically show few signs of focal cortical deficits. Preliminary indications are that language is essentially normal and measures of verbal reasoning are not severely involved (Grigsby *et al.*, 2005). The primary areas of impairment appear to be in working memory, information processing speed, declarative learning and executive cognitive functioning (ECF) (Grigsby *et al.*, 2005). This is a somewhat non-specific pattern of deficits, and while lesions of dorsolateral prefrontal cortex may result in cognitive decline in these areas of functioning, ECF is mediated by a complex network involving other structures including the anterior cingulate gyrus, cerebellum, basal ganglia and mediodorsal thalamus (Luria, 1966,1980; Stuss and Benson, 1986; Alexander and Crutcher, 1990; Fuster, 1997; Middleton and Strick, 1997; Scarnati and Florio, 1997). The loss of Purkinje cells in the cerebellum, for example, might interfere with learning and ECF (Leiner *et al.*, 1986; Schmahmann, 1991; Ivry and Baldo, 1992). Moreover, Tullberg *et al.* (2004) suggest that white matter lesions,

regardless of their location, may affect frontal lobe metabolism and the executive cognitive abilities. Finally, the significant proportion of hippocampal cells containing inclusions suggests the possibility that this pathology may be associated with memory deficits. Such problems may also be secondary to problems with working memory, or to the capacity for active learning and retrieval, affected adversely by ECF disorders.

The most striking finding of the current study is the highly significant association between the number of CGG repeats and the numbers of intranuclear inclusions in both neurons and astrocytes. An equally dramatic inverse correlation was also demonstrated between CGG repeat number and age of death. Even in this small sample of subjects, CGG repeat length appears to be a powerful predictor of neurological involvement in males, both clinically with age of death and neuropathologically with number of inclusions. It is encouraging that the lowest repeat number (65 repeats, Case 11) had mild neurological deficits that developed quite late (80s), with only a few inclusions seen post-mortem. This graded degree of clinical involvement would point to a downward estimation for the number of carriers in the general population who may develop FXTAS.

Although the precise mechanistic relationship between CGG repeat size and either inclusion formation/neuropathology or clinical involvement is still unclear, the absence of FXTAS in adults with fragile X syndrome (where the *FMR1* gene is silent) indicates that gene activity is important for disease formation and is likely a toxic gain-of-function of the *FMR1* mRNA itself (Hagerman *et al.*, 2001; Greco *et al.*, 2002; Jacquemont *et al.*, 2003; Hagerman and Hagerman, 2004). Such a gain-of-function could arise as a result of the abnormally increased levels of *FMR1* mRNA in carriers of premutation alleles (Tassone *et al.*, 2000*a*, *b*; Kenneson *et al.*, 2001) or the presence of the expanded repeat in the mRNA, or that an increasing proportion of mRNAs become extended at their 5′ ends due to a shift to transcriptional initiation further upstream with increasing CGG repeat length (Beilina *et al.*, 2004). The current study does not, however, directly address the role of *FMR1* mRNA in the pathogenesis of FXTAS. A significant correlation between mRNA levels and numbers of inclusions was only demonstrated in hilar neurons, and could therefore be due to false discovery (type I error). The apparent lack of a stronger association may be due not only to the variation in *FMR1* mRNA levels in different parts of the brain (Tassone *et al.*, 2004), but also to the fact that mRNA levels are measured in peripheral leucocytes. We were not able to obtain non-degraded (brain) *FMR1* mRNA from most of the samples, many of which were available only as fixed tissue.

Two animal systems have been developed to investigate the pathogenesis of FXTAS: a knock-in mouse model in which an expanded CGG repeat element (~100 CGG repeats) replaced the smaller CGG repeat within the homologous mouse (*Fmr1*) gene (Willemsen *et al.*, 2003) and a *Drosophila* model in which a ~90 CGG repeat was placed 5′ to an unrelated reporter gene driven by an eye-specific promoter (Jin *et al.*, 2003). There are distinct differences in the nature and distribution of inclusions between each model and FXTAS, suggesting that some aspects of the pathogenesis of FXTAS are intrinsically different from the phenotypes observed in mouse and fly. In the mouse, no inclusions are observed in astrocytes, in stark contrast to human studies where the percentages of astrocytic inclusions often outnumber corresponding numbers for neurons. If a component of FXTAS pathogenesis in humans were due to astrocytic involvement, as now seems evident, it would explain the much milder neuropathology in the mouse (Van Dam *et al.*, 2005). In the *Drosophila* model, substantial numbers of inclusions are present in the cytoplasm. In human tissue, not a single inclusion was observed in the cytoplasm in over 20 000 neuronal and astrocytic cells counted; all of the more than 1600 inclusions scored were intranuclear. Thus, although the animal models should prove useful in understanding some aspects of the pathogenesis of FXTAS, the differences suggest that at least some of the *trans*-acting factors involved in FXTAS may not be present—or functioning in the same manner—in the fly or the mouse.

The cases described in the current study display a spectrum of involvement, both clinically and neuropathologically, suggesting that additional protective and/or exacerbating factors (genetic and/or extrinsic) may modulate the effects of the CGG repeat element. One patient (Case 10), with the most rapid downhill course, also displayed features consistent with Alzheimer's disease (for more details on psychological testing see Mothersead *et al.*, 2005). Case 11 (with the smallest repeat expansion) represents an example of an older premutation carrier who manifested few of the clinical features characteristic of FXTAS. In this subject, there is little evidence of neuropathology, with only rare inclusions, and no evident cerebral or cerebellar white matter disease. Although further study is necessary to fully assess the effects of low-end premutation alleles on the eventual development of FXTAS, the current results suggest that, with many cases displaying a mild phenotype, the overall clinical prevalence of FXTAS may be significantly lower than that estimated by the overall frequency of premutation alleles.

Acknowledgements

The authors would like to thank the families whose thoughtful bequests have made this research possible. This work was supported by NICHD grants HD40661 (P.J.H.) and HD36071 (R.J.H.), by NIEHS grant P01 ES11269 (R.F.B.), by NINDS grant NS29818 (B.D.T.), by the Boory Family Fund and by the UC Davis MIND Institute for general laboratory support.

References

Alexander GE, Crutcher MD. Functional architecture of basal ganglia circuits: neural substrates of parallel processing. Trends Neurosci 1990; 13: 266–71.

Bacalman S, Farzin F, Bourgeois J, Cogswell J, Goodlin-Jones B, Gane LW, et al. Psychiatric phenotype of the fragile X-associated tremor/ataxia syndrome (FXTAS) in males: newly described fronto-subcortical dementia. J Clin Psychiatry 2005. In press.

Beilina A, Tassone F, Schwartz PH, Sahota P, Hagerman PJ. Redistribution of transcription start sites within the FMR1 promoter region with expansion of the downstream CGG-repeat element. Hum Mol Genet 2004; 13: 543–9.

Benjamini Y, Hochberg Y. Controlling the false discovery rate: a practical and powerful approach to multiple testing. J R Statist Soc 1995; 57 B: 289–300.

Berry-Kravis E, Lewin F, Wuu J, Leehey M, Hagerman R, Hagerman P, et al. Tremor and ataxia in fragile X premutation carriers: blinded videotape study. Ann Neurol 2003; 53: 616–23.

Berry-Kravis E, Potanos K, Weinberg D, Zhou L, Goetz CG. Fragile X-zassociated tremor/ataxia syndrome in sisters related to X-inactivation. Ann Neurol 2005; 57: 144–7.

Brunberg JA, Jacquemont S, Hagerman RJ, Berry-Kravis E, Grigsby J, Leehey M, et al. Fragile X premutation carriers: characteristic MR imaging findings in adult males with progressive cerebellar and cognitive dysfunction. Am J Neurorad 2002; 23: 1757–66.

Curtin F, Schulz P. Multiple correlations and Bonferroni's correction. Biol Psychiatry 1998; 44: 775–7.

Dombrowski C, Levesque S, Morel ML, Rouillard P, Morgan K, Rousseau F. Premutation and intermediate-size FMR1 alleles in 10572 males from the general population: loss of an AGG interruption is a late event in the generation of fragile X syndrome alleles. Hum Mol Genet 2002; 11: 371–8.

Fuster J. The prefrontal cortex: anatomy, physiology, and neuropsychology of the frontal lobe. Philadelphia: Lippincott-Raven; 1997.

Greco C, Hagerman RJ, Tassone F, Chudley A, Del Bigio MR, Jacquemont S, et al. Neuronal intranuclear inclusions in a new cerebellar tremor/ataxia syndrome among fragile X carriers. Brain 2002; 125: 1760–71.

Grigsby J, Brega AG, Jacquemont S, Loesch DZ, Leehey MA, Goodrich GK, et al. Impairment in the cognitive functioning of men with Fragile X Tremor-Ataxia Syndrome (FXTAS). J Neurol Sci 2005. In press.

Hagerman PJ, Hagerman RJ. The fragile-X premutation: a maturing perspective. Am J Hum Genet 2004; 74: 805–16.

Hagerman RJ, Leehey M, Heinrichs W, Tassone F, Wilson R, Hills J, et al. Intention tremor, parkinsonism, and generalized brain atrophy in male carriers of fragile X. Neurology 2001; 57: 127–30.

Hagerman RJ, Leavitt BR, Farzin F, Jacquemont S, Greco CM, Brunberg JA, et al. Fragile-X-associated tremor/ataxia syndrome (FXTAS) in females with the FMR1 premutation. Am J Hum Genet 2004; 74: 1051–6.

Ivry RB, Baldo JV. Is the cerebellum involved in learning and cognition? Curr Opin Neurobiol 1992; 2: 212–6.

Iwahashi CK, Yasui DH, An H-J, Greco CM, Tassone F, Nannen K, et al. Protein composition of the intranuclear inclusions of FXTAS. Brain 2005, Advance Access published October 24, 2005, doi:10.1093/brain/awh650.

Jacquemont S, Hagerman RJ, Leehey M, Grigsby J, Zhang L, Brunberg JA, et al. Fragile X premutation tremor/ataxia syndrome: molecular, clinical, and neuroimaging correlates. Am J Hum Genet 2003; 72: 869–78.

Jacquemont S, Farzin F, Hall D, Leehey M, Tassone F, Gane L, et al. Aging in individuals with the FMR1 mutation. Am J Ment Retard 2004a; 109: 154–64.

Jacquemont S, Hagerman RJ, Leehey MA, Hall DA, Levine RA, Brunberg JA, et al. Penetrance of the fragile X-associated tremor/ataxia syndrome in a premutation carrier population. JAMA 2004b; 291: 460–9.

Jacquemont S, Orrico A, Galli L, Sahota PK, Brunberg JA, Anichini C, et al. Spastic paraparesis, cerebellar ataxia, and intention tremor: a severe variant of FXTAS? J Med Genet 2005; 42: e14.

Jin P, Zarnescu DC, Zhang F, Pearson CE, Lucchesi JC, Moses K, et al. RNA-mediated neurodegeneration caused by the fragile X premutation rCGG repeats in Drosophila. Neuron 2003; 39: 739–47.

Kalimo H, Viitanen M, Amberla K, Juvonen V, Marttila R, Poyhonen M, et al. CADASIL: hereditary disease of arteries causing brain infarcts and dementia. Neuropathol Appl Neurobiol 1999; 25: 257–65.

Kenneson A, Zhang F, Hagedorn CH, Warren ST. Reduced FMRP and increased FMR1 transcription is proportionally associated with CGG repeat number in intermediate-length and premutation carriers. Hum Mol Genet 2001; 10: 1449–54.

Leehey MA, Munhoz RP, Lang AE, Brunberg JA, Grigsby J, Greco C, et al. The fragile X premutation presenting as essential tremor. Arch Neurol 2003; 60: 117–21.

Leiner HC, Leiner AL, Dow RS. Does the cerebellum contribute to mental skills? Behav Neurosci 1986; 100: 443–54.

Luria A. Human brain and psychological processes. New York: Harper & Row; 1966.

Luria A. Higher cortical functions in man. Vol. 2nd ed. New York: Basic Books; 1980.

Middleton F, Strick P. New concepts about the organization of basal ganglia output. In: Obeso J, DeLong M, Ohye C , Marsden C, editors. The basal ganglia and new surgical approaches for Parkinson's disease. Advances in neurology. Vol. 74. Philadelphia: Lippincott-Raven; 1997: p. 57–68.

Mothersead PK, Conrad K, Hagerman RJ, Greco CM, Hessl D, Tassone F. GRAND ROUNDS: An atypical progressive dementia in a male carrier of the fragile X premutation: An example of fragile X-associated tremor/ataxia syndrome. Appl Neuropsychol 2005; 12: 169–78.

Newell KL, Hyman BT, Growdon JH, Hedley-Whyte ET. Application of the National Institute on Aging (NIA)-Reagan Institute criteria for the neuropathological diagnosis of Alzheimer disease. J Neuropathol Exp Neurol 1999; 58: 1147–55.

Rousseau F, Rouillard P, Morel ML, Khandjian EW, Morgan K. Prevalence of carriers of premutation-size alleles of the FMRI gene—and implications for the population genetics of the fragile X syndrome. Am J Hum Genet 1995; 57: 1006–18.

Scarnati E, Florio T. The pedunculopontine nucleus and related structures: functional organization. In: Obeso J, DeLong M, Ohye C, Marsden C, editors. The basal ganglia and new surgical approaches for Parkinson's disease. Advances in neurology. Vol. 74. Philadelphia: Lippincott-Raven; 1997: p. 97–110.

Schmahmann J. An emerging concept. The cerebellar contribution to higher function. Arch Neurol 1991; 48: 1178–87.

Stuss D, Benson D. The frontal lobes. New York: Raven Press; 1986.

Tassone F, Hagerman RJ, Iklé DN, Dyer PN, Lampe M, Willemsen R, et al. FMRP expression as a potential prognostic indicator in fragile X syndrome. Am J Med Genet 1999; 84: 250–61.

Tassone F, Hagerman RJ, Chamberlain WD, Hagerman PJ. Transcription of the FMR1 gene in individuals with fragile X syndrome. Am J Med Genet 2000a; 97: 195–203.

Tassone F, Hagerman RJ, Taylor AK, Gane LW, Godfrey TE, Hagerman PJ. Elevated levels of FMR1 mRNA in carrier males: a new mechanism of involvement in the fragile-X syndrome. Am J Hum Genet 2000b; 66: 6–15.

Tassone F, Hagerman RJ, Garcia-Arocena D, Khandjian EW, Greco CM, Hagerman PJ. Intranuclear inclusions in neural cells with premutation alleles in fragile X associated tremor/ataxia syndrome. J Med Genet 2004; 41: e43.

Tullberg M, Fletcher E, DeCarli C, Mungas D, Reed BR, Harvey DJ, et al. White matter lesions impair frontal lobe function regardless of their location. Neurology 2004; 63: 246–53.

Van Dam D, Errijgers V, Kooy RF, Willemsen R, Mientjes E, Oostra BA, et al. Cognitive decline, neuromotor and behavioural disturbances in a mouse model for fragile-X-associated tremor/ataxia syndrome (FXTAS). Behav Brain Res 2005; 162: 233–9.

Willemsen R, Hoogeveen-Westerveld M, Reis S, Holstege J, Severijnen LA, Nieuwenhuizen IM, et al. The FMR1 CGG repeat mouse displays ubiquitin-positive intranuclear neuronal inclusions; implications for the cerebellar tremor/ataxia syndrome. Hum Mol Genet 2003; 12: 949–59.

Zuhlke C, Budnik A, Gehlken U, Dalski A, Purmann S, Naumann M, et al. FMR1 premutation as a rare cause of late onset ataxia–evidence for FXTAS in female carriers. J Neurol 2004; 251: 1418–9.